Re-evaluation of the ground calibration for the Arase magnetic field experiment

Mariko TERAMOTO[*1], Ayako MATSUOKA[*2], Reiko NOMURA[*3]

ABSTRACT

Herein, ground calibration experiments were performed to determine the sensitivity for all components and the angles (alignment) between the measurement axes of the magnetic field experiment (MGF) onboard Arase satellite. We can well determine the sensitivities within 0.07 % error and the alignment within 90 ± 1° with ~0.03° accuracy. Also, the temperature dependences of the offset and sensitivity were examined. Results revealed that the relative sensitivity to the room temperature can be fit with a linear regression line. The offsets exhibited systematical dependences on temperatures. Between March 13, 2017 and April 30, 2018, when MGF with an 8000-nT range mostly measured ambient magnetic field in orbit at -10°C–0°C, the linearity of sensitivity and offset with a standard error of < 0.00023 and <0.67 nT, respectively, was determined. The measured sensitivity, alignment, and offset were used to measure the magnetic field with high accuracy, thereby meeting the MGF capability and performance requirement of the field intensity <5 nT and the field direction error <1°.

Keywords: Arase (ERG) satellite, the magnetic field experiment, ground experiment for calibration

1. Introduction

The Arase (ERG) satellite, developed by the Institute of Space and Astronautical Science (ISAS)/Japan Aerospace Exploration Agency (JAXA), was successfully launched on December 20, 2016 (Miyoshi et al., 2018) [1)]. The magnetic field experiment (MGF) (Matsuoka et al., 2018)[2)] onboard the Arase was performed to record the ambient magnetic field in the region since March 2017. Table 1 lists the design specifications of the MGF that comprises a sensor (MGF-S) and an electronic box (MGF-E). To investigate the particle acceleration processes in the inner magnetosphere, Arase must measure magnetic field with the magnetic field intensity error of <5 nT and an error in its direction of <1° when the satellite is located at L > 2.

The sensitivity of the MGF can be roughly estimated using the winding number of the pickup coil of the MGF-S and resistance of the feedback resistor of MGF-E. However, the exact sensitivities for the MGF should be determined on the ground by examining its response to a calibrated magnetic field. In addition, the axes of MGF-S are not orthogonal because three sensor elements were mounted on the sensor base with slight angle mismatch. To observe the magnetic field data in the orthogonal coordinate system, the alignment of each fluxgate sensor axis in a ground experiment must be examined. The temperature dependence of sensitivity and offset of the MGF must also be evaluated because the fluxgate system has a large temperature dependency.

Before Arase was launched, Teramoto et al. (2017)[3)] determined the sensitivity and alignment of MGF-S on Arase along with the temperature dependence of the sensitivity and offset. The errors were evaluated via ground calibration experiments. MGF/Arase can obtain the actual magnetic field data for the inner magnetosphere in more than one year. Herein, the methods and results of the ground calibration experiments are summarized and the error values for the actual MGF observations are re-evaluated.

doi: 10.20637/JAXA-RR-18-005E/0001
[*] Received October 8, 2018
[*1] Institute for Space-Earth Environmental Research, Nagoya University
[*2] Department of Solar System Science, Institute of Space and Astronautical Science
[*3] Research of Interior Structure and Evolution of Solar System Bodies, National Astronomical Observatory of Japan

Table 1 MGF design specifications

sensor	ring-core
dynamic range	range-0: ±8000 nT range-1: ±60000 nT
resolution (20 bit)	range-0: 114 pT range-1: 15 pT
noise level	<10.5 pT/Hz$^{-0.5}$@1Hz
sampling rate	256 Hz

2. Ground calibration of MGF for sensor alignment and sensitivity determination

2.1. Methods

The principle and method for the ground calibration of the three-axis fluxgate magnetometer were first proposed by Acuna et al(1978)[4]. Following the method proposed by Yamamoto et al (1996)[5], we examined the output relative to the known magnetic field applied by the calibration coil. We determined the sensitivity and alignment of the magnetometer and also the direction of the calibrated magnetic field, using two orthogonal calibration mirrors.

The relationship between the relating parameters, namely the sensitivity of MGF-S [A_i(i=x,y,z)] (nT/digit), output of MGF-S [M_i] (digit), the transform matrix from the alignment mirror coordinate attached MGF-S to the sensor coordinate $\vec{\varepsilon}$, the transform matrix from the alignment mirror coordinate of the coil to the alignment mirror coordinate of the sensor [**K**], the transform matrix from the calibration coil to the calibration mirror attached calibration coil $\vec{\delta}$, the applied magnetic field [B_i] (nT), and the zero-offsets [$B_{o,i}$] (nT), is described as follows:

$$\begin{pmatrix} A_x & 0 & 0 \\ 0 & A_y & 0 \\ 0 & 0 & A_z \end{pmatrix}\begin{pmatrix} M_x \\ M_y \\ M_z \end{pmatrix} = \vec{\varepsilon}\cdot\mathbf{K}\cdot\vec{\delta}\begin{pmatrix} B_x \\ B_y \\ B_z \end{pmatrix} + \begin{pmatrix} B_{o,x} \\ B_{o,y} \\ B_{o,z} \end{pmatrix} \quad (1)$$

Equation (1) describes the applied magnetic field [B_i] and the relationship between the alignment mirror coordinates of the coil and the sensor, **K**. The output of MGF-S is known. The zero-offset of MGF-S, [$B_{o,i}$], is ignored because of the linearity between the inputs and the outputs of the applied magnetic field intensities. Thus, a total of 21 unknown parameters among [A_i], $\vec{\varepsilon}$, and $\vec{\delta}$ need to be determined.

Using the angles of the directions of the MGF-S and the calibration coil to those of calibration mirrors, as shown in Figure 1, $\vec{\varepsilon}$ and $\vec{\delta}$ are written as

$$\vec{\varepsilon} = \begin{pmatrix} 1+\varepsilon_{xx} & \varepsilon_{xy} & \varepsilon_{xz} \\ \varepsilon_{yx} & 1+\varepsilon_{yy} & \varepsilon_{yz} \\ \varepsilon_{zx} & \varepsilon_{zy} & 1+\varepsilon_{zz} \end{pmatrix} = \begin{pmatrix} \cos\theta_x\cos\phi_x & \cos\theta_x\sin\phi_x & \sin\theta_x \\ \cos\theta_y\sin\phi_y & \cos\theta_y\cos\phi_y & \sin\theta_y \\ \cos\theta_z\sin\phi_z & \sin\theta_z & \cos\theta_z\cos\phi_z \end{pmatrix} \quad (2)$$

and

$$\vec{\delta} = \begin{pmatrix} 1+\delta_{xx} & \delta_{xy} & \delta_{xz} \\ \delta_{yx} & 1+\delta_{yy} & \delta_{yz} \\ \delta_{zx} & \delta_{zy} & 1+\delta_{zz} \end{pmatrix} = \begin{pmatrix} \cos\lambda_x\cos\varphi_x & \cos\lambda_y\sin\varphi_y & \cos\lambda_z\sin\varphi_z \\ \cos\lambda_x\sin\varphi_x & \cos\lambda_y\cos\varphi_y & \sin\lambda_z \\ \sin\lambda_x & \sin\lambda_y & \cos\lambda_z\cos\varphi_z \end{pmatrix}. \quad (3)$$

$\vec{\varepsilon}$ and $\vec{\delta}$ are very close to unit matrices. Six conditions are described in (2) and (3) because the row and column vectors in $\vec{\varepsilon}$ and $\vec{\delta}$ are unit vectors, respectively.

From one experimental setup, i.e. one **K** and **B** in the x, y, and z directions, independently, nine equations can be obtained from equation (1). From the conditions obtained from (2) and (3), 15 equations in total are obtain. If the MGF-S is rotated 90° with respect to one of the coordinates, nine more equations can be obtained. However, only six equations among these nine equations are independent of the previous (un-rotated) setup. Consequently, 21 conditions are obtained in total for the 21 parameters. Although the number of conditions is sufficient to determine 21 unknown parameters, one more experimental setup (rotations of MGF-S around another axis) is required to solve the equations more reliably and stably. The alignment and sensitivity parameters are determined using the 27 conditions obtained via three-setup experiments.

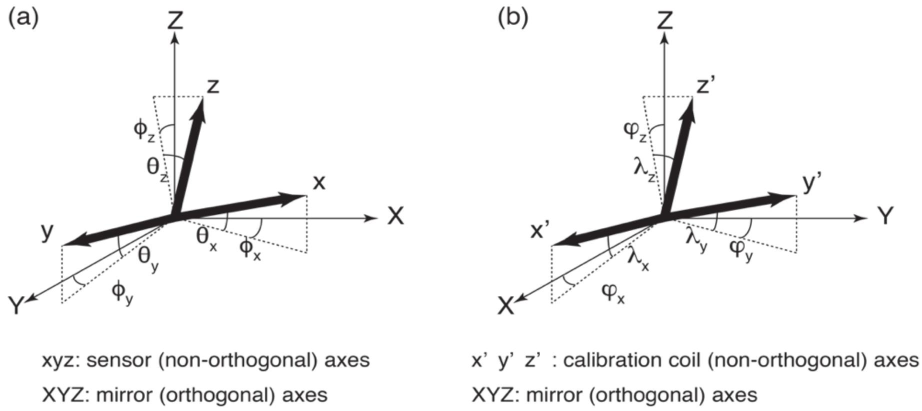

Fig. 1. Definitions of the angle (a) MGF-S and sensor mirror coordinates (b) calibration coil and coil mirror coordinates

2.2. Settings

The MGF was calibrated in the three-axis, 15-m Braunbeck coil system of the magnetic test facility at Tsukuba Space Center, JAXA, from March 2 to March 5, 2016. The Braunbeck coil system can create an almost-zero magnetic field environment in the center of this coil system by canceling the geomagnetic field and its disturbances. A three-axis Helmholtz coil system (calibration coil), which can produce the magnetic field within an accuracy of 0.1% in each direction, is installed at the center of the Braunbeck coil system to apply the magnetic field for calibration. The MGF-S on a rotation table was set at the center of the calibration coil. The cubic calibration mirrors were attached onto the calibration coil and turn table in order to setup the experiments with high accuracy using the laser alignment system.

When the **K** coordinate system of MGF-S (Figure 2) was set by rotating the table, the mirror coordinates were adjusted to match their alignment with high accuracy using the lazier alignment system installed 16 m away from the center of the calibration coil. After the mirror adjustment, the output of MGF-S was measured relative to the applied magnetic field (Table 2). The experiments were performed thrice for the ±8000-nT range and twice for ±60000-nT range at the room temperature (21.4°C).

Table 2. Applied fields during the calibration experiment

Range	Applied field (nT)
±8000-nT range	0, ±7000, ±5200, ±2600
±60000-nT range	0, ±50000 ±3000

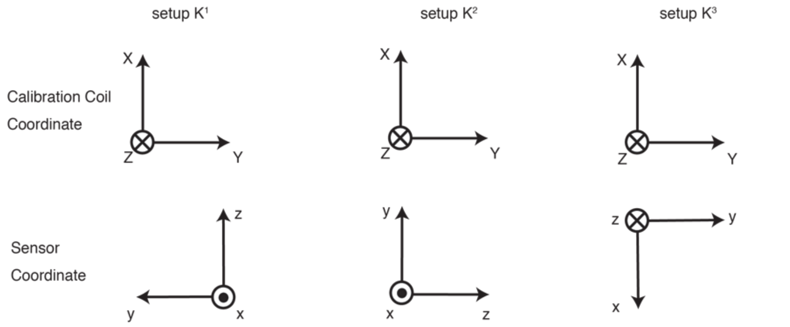

$$K^1 = \begin{pmatrix} 0 & 0 & -1 \\ 0 & -1 & 0 \\ 1 & 0 & 0 \end{pmatrix} \quad K^2 = \begin{pmatrix} 0 & 0 & -1 \\ -1 & 0 & 0 \\ 0 & 1 & 0 \end{pmatrix} \quad K^3 = \begin{pmatrix} -1 & 0 & 0 \\ 0 & 1 & 0 \\ 0 & 0 & 1 \end{pmatrix}$$

Fig. 2. Configurations of the coil and the sensor

2.3. Results

Figure 3 shows an example of the MGF output (M_i) relative to the applied magnetic field (*Bi*) (K1, K2, or K3) for one experiment. Mi is the 10-s averaged data. As expected in equation (1), we find clear linearities between the input and output magnetic fields. We confirmed that such linearity holds for all experiments with ±8000-nT and ±60000-nT ranges. The output matrix **M** in the equation (1) is obtained from the inclination of the M relative to B. The standard errors between regression lines and the measurements are within 0.05% for all experiments.

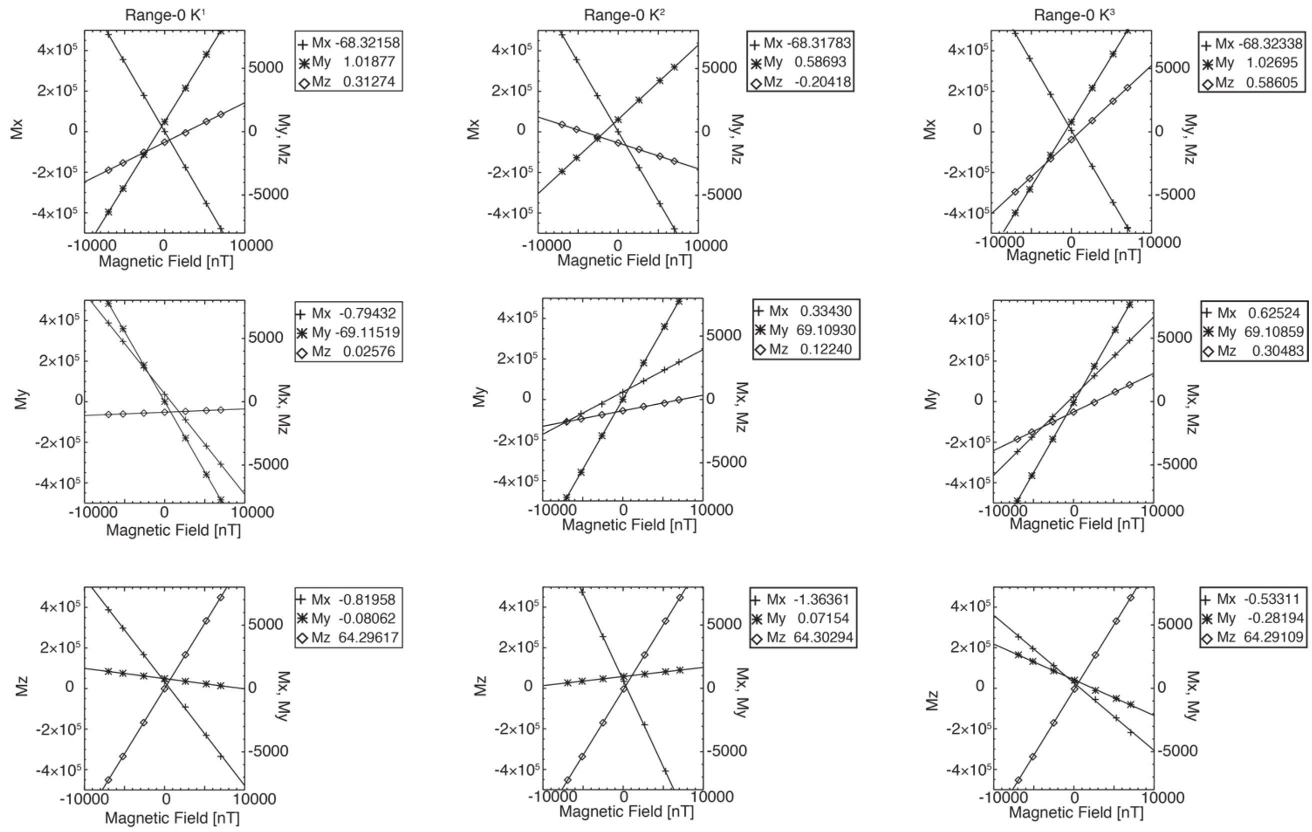

Fig.3 Output M relative to the applied magnetic field B within 8000-nT range

2.3.1. Sensitivity

Table 3 shows the sensitivities and the relative errors in the 60000-nT and 8000-nT ranges obtained from the equations (1), (2), and (3). The sensitivities of both ranges were well determined with an error of < 0.07 %. The maximum error of 0.06 % with the 8000-nT range indicates that the analytical errors are <4.8 nT when MGF is used to observe magnetic field at the intensity of 8000 nT, which is within the required error of 5 nT for Arase.

Using the actual magnetic field data measured in the magnetosphere by MGF with the ±8000-nT range from March 13, 2017 to April 30, 2018, we investigated the magnetic field intensity measured by Arase. We found that the magnetic field intensities measured by MGF (with the 8000 nT range) are at less than 1000 nT in most cases: at 91.0%, 91.3 %, and 90.3% of the total measurement time for X, Y, and Z components respectively. This result indicates that the analytical error of MGF due to determination of sensitivity is less than 0.6 nT. We conclude that most of the 8000nT range measurements meet the observational requirement for Arase.

Table 3. Sensitivity of MGF-S/Arase

	X component		Y component		Z component	
	Sensitivity (nT/digit)	Error (%)	Sensitivity (nT/digit)	Error (%)	Sensitivity (nT/digit)	Error (%)
60000-nT range	0.1072	0.03	0.1057	0.07	0.1137	0.04
8000-nT range	0.01464	0.06	0.01447	0.06	0.01555	0.05

2.3.2. Alignment of the MGF-S

The determined angles between the MGF-S and calibration mirror alignments with each range are summarized in Tables 4. While ϕ_x, ϕ_y, ϕ_z , and θ_z of the 8000-nT range are almost similar to those of the 60000-nT range, θ_x and θ_y for the 8000-nT range are respectively 0.57° and 0.08° smaller than those of the 60000-nT range. Due to the differences in these angles, Y-Z and Z-X angles of the 8000-nT range are 0.1° and 0.54° larger than those of the 60000-nT range, respectively, as shown in Table 5. Thus, a different alignment must be applied for each range when we calibrate the in-flight data of MGF in orbit. As shown in Table 4, we can determine the alignment with a high accuracy, i.e., the estimated error is <0.03° for both ranges.

In addition to the analytical error of the abovementioned alignments, we need to evaluate the alignment error from the experimental equipment. The coordinate system of MGF-S has an alignment error within 0.03° relative to the calibration coil because the plane of turn table, onto which MGF-S and the calibration mirror were attached, has a slight difference from the horizontal. Further, the adjustment of the coordination system using the laser system has the alignment error within the 0.03°. Thus, the alignment error from the experiment equipment is <0.07°. Even though the additional error from the experimental equipment is included in the total alignment error, we determined the alignment error to be <0.1°, which is sufficient to meet the observational requirements.

Table 4. Obtained angles for sensor-mirror alignment. Unit is degrees

	θ_x	ϕ_x	θ_y	ϕ_y	θ_z	ϕ_z
60000-nT range	-0.15 ± 0.03	0.23 ± 0.003	0.26 ± 0.004	-0.43 ± 0.01	-0.12 ± 0.02	-0.26 ± 0.01
8000-nT range	-0.72 ± 0.02	0.25 ± 0.03	0.18 ± 0.004	-0.44 ± 0.006	-0.15 ± 0.006	-0.23 ± 0.03

Table 5. Angle between the axes. Unit is degrees

	∠XY	∠YZ	∠ZX
60000nT range	90.20	89.86	90.41
8000nT range	90.19	89.97	90.95

2.3.3. Alignment of the calibration coil

The obtained angles between the calibration coil and calibration mirror alignments and the relative angles between axes of calibration coil are summarized in Tables 6 and 7, respectively. The obtained and relative angles do not show significant differences between different ranges. The relative angles are within 0.01°, indicating that the relative angles of the calibration coil are estimated with high accuracy.

Table 6. Obtained angles for coil-mirror angle. Unit is degrees.

	ψ_x	λ_x	ψ_y	λ_y	ψ_z	λ_z
60000-nT range	-0.04 ± 0.02	0.44 ± 0.001	0.42 ± 0.02	-0.29 ± 0.06	-0.42 ± 0.001	0.06 ± 0.05
8000-nT range	-0.04 ± 0.007	0.42 ± 0.002	0.42 ± 0.006	-0.28 ± 0.02	-0.41 ± 0.002	0.05 ± 0.04

Table 7. Angle between axes of calibration coil. Unit is degrees.

	∠XY	∠YZ	∠ZX
60000-nT range	89.86	89.99	89.98
8000-nT range	89.86	89.99	89.99

3. Temperature dependence of the sensitivity and offset

3.1. Methods

We can derive the temperature dependence of the sensor by measuring the output of the MGF, $\mathbf{M}_{\mathbf{app}}$, before and after applying external magnetic field, $\mathbf{B}_{\mathbf{app}}$, with a Helmholtz coil in a space, which is left approximately zero ($\mathbf{B}_{\mathbf{env}}$). Given that the output, offset, and sensitivity at room temperature (and at a temperature *t*) are $\mathbf{M}_{\mathbf{app,o}}$ ($\mathbf{M}_{\mathbf{app,t}}$), and $\mathbf{M}_{\mathbf{0,o}}$ ($\mathbf{M}_{\mathbf{0,t}}$), and $\mathbf{a}_{\mathrm{o}}$($\mathbf{a}_{\mathrm{t}}$) respectively, $\mathbf{M}_{\mathrm{app,o}} = \mathbf{a}_{\mathbf{o}} (\mathbf{B}_{\mathbf{app}}+\mathbf{B}_{\mathbf{env}}) + \mathbf{M}_{\mathbf{0,o}}$ and $\mathbf{M}_{\mathbf{app,t}} = \mathbf{a}_{\mathrm{t}} (\mathbf{B}_{\mathbf{app}}+\mathbf{B}_{\mathbf{env}}) + \mathbf{M}_{\mathbf{0,t}}$. Therefore, the relative sensitivity of a temperature (t) to room temperature is given as

$$\frac{\mathbf{a}_t}{\mathbf{a}_\mathbf{o}} = \frac{\mathbf{M}_{\mathbf{app,t}} - \mathbf{M}_{\mathbf{0,t}}}{\mathbf{M}_{\mathbf{app,o}} - \mathbf{M}_{\mathbf{0,o}}} \tag{4}$$

The offset of the MGF-S is obtained by the output in both the normal and the reverse directions in the stably almost-zero magnetic field ($\mathbf{B}_{\mathbf{env}}$). Given that the MGF-S outputs in the normal and reverse directions at the temperature of *t* are

$$\mathbf{M}_{\mathbf{n,t}} = \mathbf{a}_{\mathbf{t}}\mathbf{B}_{\mathbf{env}} + \mathbf{M}_{\mathbf{0,t}} \tag{5}$$

$$\mathbf{M}_{\mathbf{r,t}} = -\mathbf{a}_{\mathbf{t}}\mathbf{B}_{\mathbf{env}} + \mathbf{M}_{\mathbf{0,t}} \tag{6}$$

the offset at a certain temperature is obtained by

$$\mathbf{M}_{\mathbf{0,t}} = \frac{\mathbf{M}_{\mathbf{n,t}} + \mathbf{M}_{\mathbf{r,t}}}{2} \tag{7}$$

We can estimate temperature dependence of relative sensitivity and offset of the MGF-S, by measuring $\mathbf{M}_{\mathbf{n,t}}$, $\mathbf{M}_{\mathbf{r,t}}$, and $\mathbf{M}_{\mathbf{app,t}}$ at various temperature around the MGF-S.

3.2. Setting

The temperature experiment was performed from February 8 to February 12, 2016 in a magnetic shielding chamber at ISAS, JAXA. The magnetic field in this chamber made of triple-layer permalloy is stably <30 nT. We used the similar equipment and method as the temperature experiments for MMO/MGF[6]. The three coils of MGF-S detached from the pedestal were installed in parallel to each other on a ceramic disk. The two thermopiles for monitoring temperature around the MGF-S was attached to the disk across the MGF-S. We controlled temperature in the thermos bottle with a ceramic lid, in which the disk was confined. This thermos bottle was placed between the applied coils which induced the magnetic field around the MGF-S with a 20-mA current. The thermos bottle and the applied coils were placed a turn table, by which MGF-S can be rotated and reversed.

In higher-temperature measurements, we heated the thermos bottle to 45°C using a heat gun. After keeping the thermos bottle at 45°C for 30 min, the heat gun was removed from the thermos bottle; then, the experiment was performed as the ambient temperature in the bottle decreased by 5°C. In the low-temperature measurements, the bottle was cooled using dry ice. After stuffing 90-g crushed dry ice uniformly between the bottle and the disk, measurements were performed (at every 5°C interval) when the temperature in the bottle began increasing.

When the temperature in the bottle increases or decreases by 5°C, we measured the temperature and the output of MGF-S for the following three situations :(a) at the normal position with no applied magnetic field; (b) at the normal position with an applied magnetic field; and (c) at the reverse position with no applied magnetic field, as illustrated in Figure 4. In situation (a), each component of MGF-S measured an ambient magnetic field of <30 nT in the magnetic shield chamber. These outputs correspond to $\mathbf{M}_{n,t}$. In situation (b), MGF-S observed the total magnetic field of the ambient magnetic field in the chamber and the applied magnetic field generated by the calibration coil. This output is $\mathbf{M}_{app,t}$. Rotating the turn table horizontally by 180°, we set the MGF-S for the situation (c). The MGF-S observed the ambient magnetic field of the magnetic shielding room in the opposite direction to one in the situation (a). This output corresponds to $\mathbf{M}_{r,t}$.

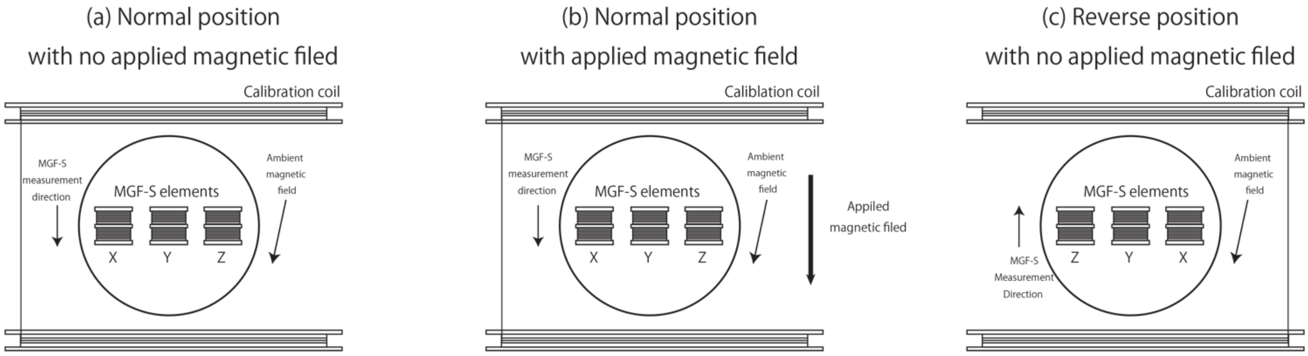

Fig 4. Each position of the MGF-S in the temperature experiments

3.3. Results

We performed temperature experiments thrice (Experiments 1, 2, and 3) within -20°C–30°C, which is expected temperature range for the MGF observation in the inner magnetosphere. We used the 8-s average outputs of the MGF with the-8000 nT range.

3.3.1. Relative sensitivities

Figure 5 represents the temperature dependences of the relative sensitivities in X, Y, and Z components of MGF-S. We only showed the measurements from Experiment 1, in which the dispersions of the measurements from the liner regression model is the smallest among all the experiments. We determined the following linear expressions from the measurements in Experiment 1 as

$$
\begin{aligned}
r_x &= 4.8577 \times 10^{-5} t + 0.99876 \\
r_y &= 4.9017 \times 10^{-5} t + 0.99878 \\
r_z &= 4.2169 \times 10^{-5} t + 0.99998
\end{aligned} \tag{8}
$$

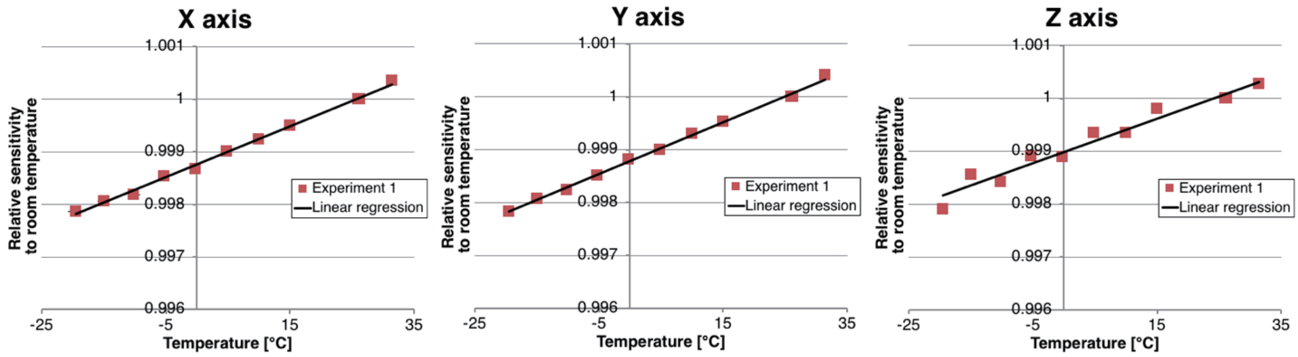

Fig. 5. Temperature dependence of sensitivity. Ratio to the sensitivity to the room temperature 26.1 °C is shown

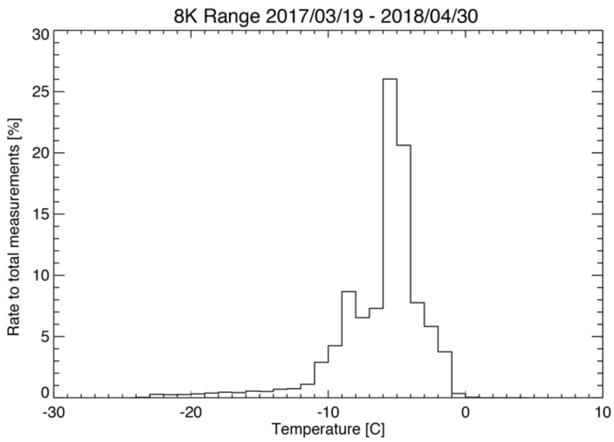

Fig. 6. Histogram of the rate of total measurements of MGF 8000-nT range between March 19, 2017 and April 30, 2018

Then, we considered the errors of the sensitivity applying temperature dependence as expressed as (8). Tables 8 and 9 represent the standard errors from the regression lines and the measurement errors of the MGF for the observations of the 8000-nT ambient magnetic field. The standard error of the Z component of the MGF (1.3 nT in the 8000-nT magnetic field intensity) is the largest among all the components between -20°C and 30°C.

In the in-flight measurements, the temperatures of the MGF-S are expected to be mostly higher than -10°C, except for the case with the long-term shading. Figure 6 represents the histogram of the MGF-S temperature with a bin width of 1°C when the MGF measured magnetic field in flight with 8000-nT range from March 19, 2017 to April 30, 2018. As expected, 91.1%, of MGF data were obtained between -10°C and 0°C.

As shown in Tables 8 and 9, we evaluated the standard errors of the temperature dependence of the sensitivity in three categories: from -20°C to -10°C, from -10 to 0°C, and from 0°C to 30°C. The standard errors of the relative sensitivities in all components decrease as the temperature increases. Table 8 shows that the standard error from the regression lines is less than 0.00023 between -10°C and 0°C. As shown in Table 9, the uncertainty due to the temperature dependence within -10°C–0°C is <1.9 nT when the MGF observed the magnetic field intensity of 8000 nT. The uncertainty due to the temperature dependence sufficiently matches the requirements of Arase.

Table 8. Standard errors for temperature dependence.

	X	Y	Z
-20°C–30°C	$\pm 7.9943 \times 10^{-5}$	$\pm 5.8729 \times 10^{-5}$	$\pm 1.6558 \times 10^{-4}$
-20°C–-10°C	$\pm 1.7606 \times 10^{-4}$	$\pm 6.1742 \times 10^{-5}$	$\pm 3.8642 \times 10^{-4}$
-10°C–0°C	$\pm 1.0387 \times 10^{-4}$	$\pm 6.5215 \times 10^{-5}$	$\pm 2.3393 \times 10^{-4}$
0°C–30°C	$\pm 7.2412 \times 10^{-5}$	$\pm 7.3208 \times 10^{-5}$	$\pm 1.5327 \times 10^{-4}$

Table 9. Uncertainty due to the temperature dependence for 8000 nT.

	X	Y	Z
−20°C–30°C	±0.64	±0.47	±1.3
−20°C–−10°C	±1.4	±0.49	±3.1
−10°C–0°C	±0.83	±0.52	±1.9
0°C–30°C	±0.58	±0.59	±1.2

3.3.2. Offset

Figure 7 shows the temperature dependence of the offset for each component, of which outputs are applied by sensitivity determined in Section 2.3.1 at 21.4°C and the temperature dependence as expressed as (8) and converted to physical value. While the offset seems to have some systematical dependences on temperature, it is difficult to find an ideal model to fit the experimental results with high accuracy. We determined the offset by averaging the experimental results, dividing temperature to three categories as mentioned in the previous sub-sections. The averaged offsets are 8.18, 10.5, and -10.6 nT for X, Y, and Z components, respectively, within -10°C–0°C, at which the MGF mostly obtains magnetic field data for the inner magnetosphere. The standard error analysis indicates that the determined offset of MGF-S has an uncertainty of <0.67 nT, which meets the requirement of MGF.

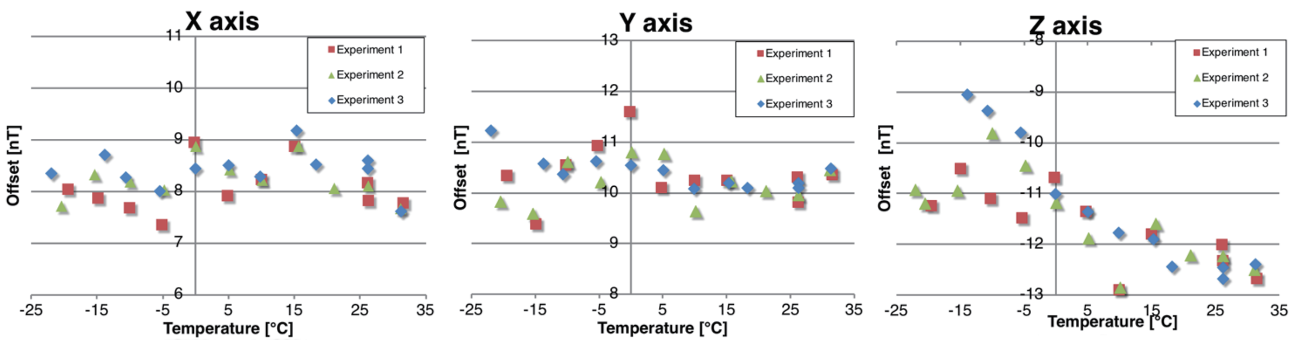

Fig. 7. Temperature dependence of the offset

Table 10. Averages and standard error of the offset in each directions of the MGF-S sensor.

	X		Y		Z	
	Averaged Offset	Standard Error	Averaged Offset	Standard Error	Averaged Offset	Standard Error
−20°C–30°C	8.23	±0.36	10.3	±0.44	−11.5	±0.56
−20°C–−10°C	8.04	±0.44	10.4	±0.67	−10.4	±0.97
−10°C–0°C	8.18	±0.54	10.5	±0.63	−10.6	±0.67
0°C–30°C	8.41	±0.36	10.2	±0.25	−12.0	±0.59

4. Summary and conclusion

Ground experiments were performed to obtain sensitivity and alignment data for the MGF onboard the Arase satellite and evaluated whether the determined sensitivity and alignment meet the scientific requirements for the Arase observation. The sensitivities for all component were determined in the 8000-nT and 60000-nT ranges with high accuracy using the method proposed by Yamamoto et al (1996)[5]. The analytical error of MGF sensitivity in the 8000-nT range is less <0.06%. Because MGF mostly operates in 8000-nT range at magnetic intensities of <1000nT, the magnetic intensities observed using MGF for each component have errors <0.6nT. The sensor axes are orthogonal to each other within 0.95° with an estimated error of <0.07°.

The temperature dependence of sensitivity and offset were also determined. Within -10°C–0°C, in which MGF mostly measured the magnetic field from March 13, 2017 to April 30, 2018, the sensitivities had a linearity to the temperature with a standard error of <0.00023. It indicates that in the 8000-nT range the MGF mostly observed the magnetic field with an uncertainty of <1.9 nT due to temperature dependence. The offset of the sensors has no clear linearity but reproducibility against temperature. The averaged offsets in the temperature from -10°C to 0°C are 8.18, 10.5, and -10.6 nT for the X, Y, and Z components, respectively. We can determine these offsets with a standard error of <0.67 nT.

These ground examinations show that the determination accuracies of the amplitude and direction of the magnetic field observed using the Arase/MGF satisfy the requirements for the Arase observations.

ACKNOWLEDGEMNETS

We are grateful for the manufacturers of MGF (Sumitomo Heavy Industries, Ltd. and Tierra Tecnica Corporation) and the extendable MAST (NIPPI Corporation). The MGF calibration test was supported by the Environment Test Technology Unit of JAXA. Science data of the Arase (ERG) satellite were obtained from the ERG Science Center operated by ISAS/JAXA and ISEE/Nagoya University (https://ergsc.isee.nagoya-u.ac.jp/index.shtml.en). The MGF v01.01 data were analyzed in this study. Studies of M.T. were partly conducted at the ERG Science Center.

REFERENCE

[1]Miyoshi, Y., Shinohara, I., Takashima, T., Asamura, K., Higashio, N., Mitani, T., Kasahara, S., Yokota, S., Kazama, Y., Wang, S.-Y., Tam, S.W.Y., Ho, P.T.P., Kasahara, Y., Kasaba, Y., Yagitani, S., Matsuoka, A., Kojima, H., Katoh, Y., Shiokawa, K., and Seki, K., Geospace exploration project ERG, Earth, Planets and Space, 70:101 (2018).

[2]Matsuoka, A., Teramoto, M., Nomura, R., Nose, M., Fujimoto, A., Tanaka, Y., Shinohara, M., Nagatsuma, T., Shiokawa, K., Obana, Y., Miyoshi, Y., Mita, M., Takashima, T., and Shinohara, I., The ARASE(ERG) magnetic field investigation, Earth, Planets and Space, 70:43 (2018).

[3]Teramoto, M., Matsuoka, A., and Nomura, R., Ground calibration experiments of Magnetic field experiment on the ERG satellite, JAXA-RM-16-003 (2017).

[4]Acuna, M.H., MAGSAT–Vector Magnetometer Absolute Sensor Alignment Determination, NASA Goddard Space Flight Center X-754-83-9 (1978).

[5]Yamamoto, T., Kokubun, S., and GEOTAIL/PLANET-B MGF team, Ground Calibration of High-Sensitivity Magnetometers for Spacecraft Use, The Institute of Space and Astronautical Report, 88 (1996).

[6]Nishio, A., Usui, M., Tohyama, F., and Matsuoka, A., Wide-Temperature-Range Test of Fluxgate Magnetometer Sensor for Mercury Exploration, Proceeding of the School of Engineering of Tokai University, Vol. 46, No. 2 (2006), pp.123-128.